DESIGN AND DISPATCH OF DECENTRALIZED ENERGY SYSTEMS USING ARTIFICIAL NEURAL NETWORKS

Lukas Koenemann[1,2], Astrid Bensmann[1,*], Johannes Gerster[2], Richard Hanke-Rauschenbach[1]

[1]Leibniz University Hannover, Institute of Electric Power Systems, Appelstraße 9A, 30167 Hannover, Germany
[2]WETEC Systems GmbH, Heerstraße 23, 45478 Mülheim an der Ruhr, Germany

*Corresponding Author: astrid.bensmann@ifes.uni-hannover.de

ABSTRACT

Decentralized energy systems, pivotal in transitioning towards a sustainable energy future, require intelligent dispatch strategies for the operation of flexible components in order to integrate inflexible renewable energy sources economically. Conventional rule-based dispatch strategies often fail to optimally exploit the capabilities of flexible system components, while optimal dispatch models, based on the assumption of perfect forecasting, tend to overestimate their performance. This paper investigates the effectiveness of artificial neural networks (ANNs) as a dynamic dispatch strategy for distributed energy systems (DES), evaluating their performance in operational scenarios with a predefined system layout and during the system design optimization phase.

Our analysis shows that ANN-based dispatch strategies outperform conventional rule-based methods by up to 8.19% in operational efficiency according to training datasets and by 3.19% in validation datasets. However, they fall short of optimal dispatch strategies by 4.52% and 1.59% in training and validation datasets, respectively. When applied to system design optimization, ANN-based strategies outperform rule-based approaches by 5.80-9.19% but underperform against optimal dispatch designs by 10.63%. Crucially, the study highlights that dispatch strategies not only influence overall system costs but also significantly impact the sizing and configuration of individual system components. This underlines the importance of incorporating intelligent dispatch strategies like ANNs early in the design process to ensure a balanced and cost-effective system architecture.

1 INTRODUCTION

The subject of the present paper is to address the design and dispatch of Decentralized Energy System (DES) using Artificial Neural Networks (ANN). The global energy supply paradigm shift toward a more sustainable and renewable depends on DES. These systems are essential for increasing efficiency, lowering dependency on traditional energy infrastructures, and locally integrating renewable energy sources. Therefore, DES need dispatchable energy converters, storage units, or consumers to incorporate inflexible renewable energies as locally and effectively as possible (Reynolds et al., 2019). The full potential of these sophisticated and expensive systems is often not realized with conventional dispatch strategies, such as predetermined priority order lists, and is often overestimated by optimal dispatch. This highlights the necessity of more innovative approaches, such as ANN or model-predictive control, for the best possible system operation. Because system design and operation are highly interdependent, these novel dispatch strategies must be considered from the outset of the design process to account for dispatchable and renewable components properly (Perera et al., 2020).

https://doi.org/10.52202/077185-0198

In the past, rule-based dispatch strategies have been widely used in DES, especially those that rely on conventional power supply and where flexibility is less important. The range of rule-based dispatch systems includes basic priority order lists (e.g. Wilke, 2020), more complicated rule sets like load-following strategies (e.g. Urbanucci and Testi, 2018), and fuzzy logic approaches (e.g. Perera et al., 2019). Rule-based dispatch strategies have the benefit of being able to be employed in real-time operations and being frequently simple to build. However, a unique set of rules based on expert knowledge must be developed for every energy system individually. In the design phase, when the system layout and component design have to be chosen, this can be challenging and may result in sub-optimal operation and system designs.

Conversely, mathematical dispatch optimization offer theoretical optimal solutions but are generally constrained to offline applications due to their reliance on perfect forecasts. Recent studies have proposed various optimization models, from linear programming (e.g. Murray et al., 2019) to more complex mixed-integer nonlinear programming solutions (e.g. Schmeling et al., 2022), aimed at unifying the design and operational aspects of DES. Because these approaches assume perfect prediction, they overestimate the behavior of flexible components, which can lead to sub-optimal sizing. Model predictive control offers the possibility of optimal operation and, simultaneously, the possibility of real-time application due to the consideration of limited forecast knowledge. For example, Stadler et al. (2016) presents a two-stage, multi-criteria optimization approach for dimensioning thermal and electrical energy systems, considering optimal operation based on a model predictive structure.

ANNs offer the possibility of mapping mathematical functions of any kind (Cybenko, 1989). For this reason, they are already being used in various areas of energy system analysis, e.g., in weather and load forecasting (e.g. Reynolds et al., 2019), fault and defect detection (e.g. Rahman Fahim et al., 2020), surrogate modeling (e.g. Geyer and Singaravel, 2018), and in building control (e.g. Wang and Hong, 2020). However, they are used to dispatch DES directly as well. Domínguez-Barbero et al. (2020) uses a deep Q-Network, an ANN with discrete action spaces, to dispatch a microgrid with a lithium-ion battery and hydrogen storage. Jin et al. (2022) and Qiu et al. (2023) employed a deep deterministic policy to dispatch renewable-based energy systems. These studies have shown that ANN-based dispatch strategies are competitive with alternative approaches. Perera et al. (2019) explored the possibility of using ANN-based dispatch in the system design process. The ANN-based design improved goal values by 60–80% compared to a presented fuzzy logic approach.

The exploration of ANNs for the dispatch of DES marks a significant leap forward, showcasing the potential of this technology in enhancing system efficiency and adaptability. However, the majority of existing research focuses on the operational aspect, leaving a gap in integrating ANN-based dispatch strategies during the system design optimization. The present study investigates the influence of dispatch strategy on the operation and optimal design of DES, focusing on the dispatch with ANNs. For this purpose, different dispatch strategy approaches, including two rule-based, an optimal dispatch and an ANN-based approach, are first introduced and compared in a case study using an already designed system. The different dispatch strategy approaches are then applied to the system optimization, and the influence of the dispatch strategy on the system design is investigated.

The present paper is organized as follows: Section 2 provides an overview of the system optimization model under consideration. Section 3 introduces the training framework for the ANN-based dispatch strategy. Section 4 presents a comparative analysis of ANN-based strategies against conventional approaches through a case study examining fixed and optimized system designs. Finally, section 5 offers concluding remarks, summarizing our research's key findings.

2 MODEL DESCRIPTION

This section provides an overview of the energy system under consideration, including the optimization problem, the component models, and the benchmark dispatch strategies.

https://doi.org/10.52202/077185-0198

2.1 System optimization problem

The structure of the system optimization problem is depicted in Figure 1. System optimization aims to minimize Total Annual Cost J (TAC) by optimizing the design $\mathbf{x}_{\text{design}}$ of the components: A Photovoltaic system (PV), a Li-ion Battery storage (B), a Heat Storage (HS), a Heat Pump (HP) and an Electric Boiler (EB). A dispatch strategy is required to operate the various system components. This may include additional optimization variables $\mathbf{x}_{\text{dispatch}}$ to be determined during system optimization. Since storage units are included in the energy system, the initial State of Energy (SOE) levels $\mathbf{x}_{\text{start}}$ must also be optimized.

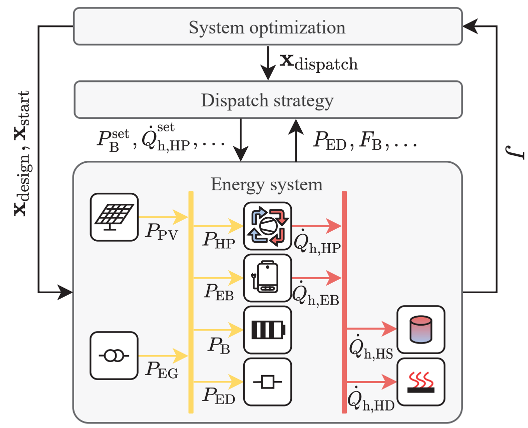

Figure 1: Structure of the system optimization problem considering an energy system with a photovoltaic system P_{PV}, a Li-ion battery P_{B} and an electrical grid connection P_{EG} for electrical supply, and a heat pump $\dot{Q}_{\text{h,HP}}$, an electric boiler $\dot{Q}_{\text{h,EB}}$ and a heat storage $\dot{Q}_{\text{h,HS}}$ for heat supply.

The detailed description of the system optimization problem is given below:

$$\underset{\mathbf{x}_{\text{design}},\mathbf{x}_{\text{dispatch}},\mathbf{x}_{\text{start}}}{\text{minimize}} \quad J \tag{1}$$

$$\text{subject to} \quad 0 = -P_{\text{ED}} + P_{\text{EG}} + P_{\text{PV}} - P_{\text{HP}} - P_{\text{EB}} - P_{\text{B}}, \tag{2}$$

$$0 = -\dot{Q}_{\text{h,HD}} + \dot{Q}_{\text{h,HP}} + \dot{Q}_{\text{h,EB}} - \dot{Q}_{\text{h,HS}}, \tag{3}$$

$$F_{\text{B,end}} \geq F_{\text{B,start}}, \tag{4}$$

$$T_{\text{HS,end}} \geq F_{\text{HS,start}}, \tag{5}$$

$$\text{eqs. (6) - (20)}$$

The TAC is calculated by considering the following parts: The annual capital and maintenance cost $J_{\text{c,m}}$, and the annual operating cost J_{o}:

$$J = J_{\text{c,m}} + J_{\text{o}} \tag{6}$$

The annuity method is used to calculate the annual capital and maintenance cost of the components:

$$J_{\text{c,m}} = \sum_{j \in \{\text{PV, B, HP, EB, HS}\}} I_j \cdot a_j \cdot (1 + c_{\text{m},j}), \tag{7}$$

where I_j is the total acquisition cost, $c_{\text{m},j}$ is the specific maintenance cost, and a_j is the annuity payment factor. The annuity payment factor can be calculated using the component life span T_j and the imputed interest rate (assumed to be 3.5%). The total acquisition cost

$$I_j = x_{\text{design},j} \cdot c_{\text{acq,var},j} + \begin{cases} c_{\text{acq,fix},j} & \text{if } x_{\text{design},j} > x_{\text{design},j}^{\min} \\ 0 & \text{else} \end{cases} \tag{8}$$

https://doi.org/10.52202/077185-0198

are split into the specific acquisition cost $c_{\text{acq,var},j}$ dependent on the sizing variable $x_{\text{design},j}$ and fixed acquisition cost $c_{\text{acq,fix},j}$ for installing a component with the minimum size $x^{\text{min}}_{\text{design},j}$. For the annual operating costs of the system, only the income from the feed-in tariff and the costs from grid procurement are considered:

$$J_{\text{o}} = \int \underbrace{p_{\text{energy}} \cdot P_{\text{EG}} \cdot H\left(P_{\text{EG}}\right)}_{\text{Energy import cost}} + \underbrace{p_{\text{feed-in}} \cdot P_{\text{EG}} \cdot H\left(-P_{\text{EG}}\right)}_{\text{Feed-in revenue}} \mathrm{d}t, \tag{9}$$

where p_{energy} is the grid purchase price, $p_{\text{feed-in}}$ is the feed-in tariff and H is the Heaviside function. According to the German market regulation, the feed-in tariff is assumed to be 5.83 ct/kWh (Federal Government Germany, 2016), and the grid purchase price is assumed to be 48.12 ct/kWh (Bundesverband der Energie- und Wasserwirtschaft, 2023). The electrical grid power P_{EG} results directly from the electrical power balance (cf. eq. 2). In addition to the electrical power balance, the optimization is also constrained by the heat power balance (cf. eq. 3), the cyclic boundary condition for the storage units' SOE (cf. eqs. 4 and 5), and the subsequent system of equations for the component models and the considered dispatch strategy. The mathematical model is implemented in the equation-based modeling language

Table 1: Component-specific economic parameters used in the case study.

Parameter	Photovoltaic	Battery	Heat pump	Electric boiler	Heat storage
$c_{\text{acq,var}}$	1075 EUR/kW[1]	500 EUR/kWh[1]	629 EUR/kW[2]	253 EUR/kW[2]	850 EUR/m^3[2]
$c_{\text{acq,fix}}$	0 EUR[1]	0 EUR[1]	5661 EUR[2]	760 EUR[2]	2125 EUR[2]
c_{m}	0.02[1]	0.02[1]	0.015[2]	0.01[2]	0.013[2]
T_{life}	30 a[1]	15 a[1]	18 a[2]	30 a[2]	17.5 a[2]

1: Kost (2021)
2: Ministerium für Umwelt, Klima und Energiewirtschaft Baden-Württemberg (2023)

Modelica using the open-source software framework *Open Modelica* (Open Source Modelica Consortium, 2022) and the optimization is performed using the *particle swarm optimization* algorithm from *pygmo* (python parallel optimization library) (Biscani and Izzo, 2010).

2.2 System component models

The mathematical equations for the system components are introduced in the following section. The associated component parameters for the case study can be found in Table 2.

2.2.1 Energy source and demand: The photovoltaic system is modeled as an inflexible energy source. The normalized power u_{PV} is calculated in advance using the method of Pfenninger and Staffell (2016) and scaled by the rated power $P^{\text{rated}}_{\text{PV}}$, which serves as the design variable of the PV system:

$$P_{\text{PV}} = u_{\text{PV}} \cdot P^{\text{rated}}_{\text{PV}}. \tag{10}$$

The district's energy needs consist of electricity and heat for hot water and heating. The method of McKenna and Thomson (2016) is used to calculate the consumption of around 15 households. In the following analyses, Kotzur et al. (2018) method is used to calculate six independent typical periods from the year-round profiles to reduce the calculation time. Figure 2 shows the pre-calculated typical period profiles for the normalized photovoltaic power, the ambient temperature, and the electrical and thermal demand. In addition to the original year-round profile, a test data set is created using the abovementioned methods.

2.2.2 Energy converter: Both energy converters - an air-source heat pump and an electric boiler - are modeled using a performance model to calculate the input/output behavior

$$\dot{Q}_{\text{h},j} = \eta_j \cdot P_j \tag{11}$$

https://doi.org/10.52202/077185-0198

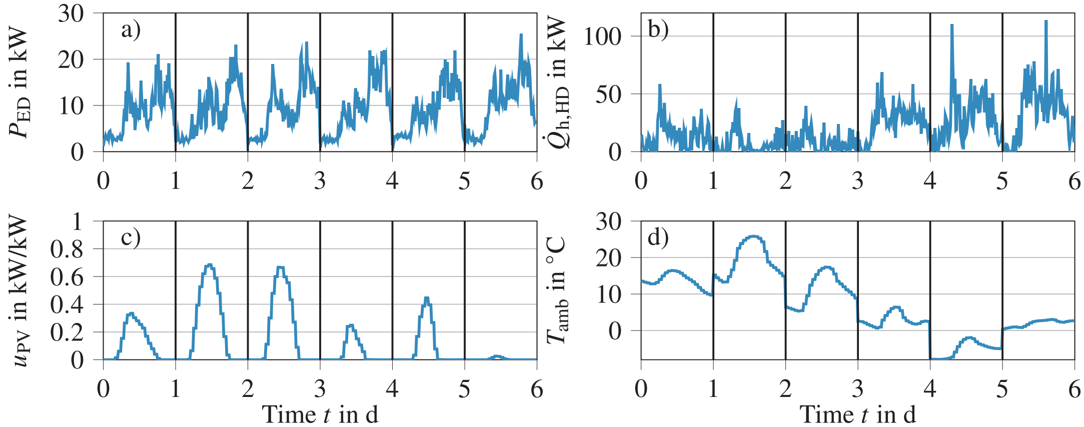

Figure 2: The imputed time series for a) electric demand P_{ED}, b) heat demand $\dot{Q}_{\mathrm{h,HD}}$, c) normalized photovoltaic power u_{PV}, and d) ambient temperature T_{amb}.

and a component management system to consider the operating limits:

$$\dot{Q}_{\mathrm{h},j} = \begin{cases} \dot{Q}^{\mathrm{set}}_{\mathrm{h},j} & \text{if } T_{\mathrm{amb}} > T^{\mathrm{cut-off}}_{j} \wedge 0 \le \dot{Q}^{\mathrm{set}}_{\mathrm{h},j} < \dot{Q}^{\mathrm{rated}}_{\mathrm{h},j} \\ \dot{Q}^{\mathrm{rated}}_{\mathrm{h},j} & \text{if } T_{\mathrm{amb}} > T^{\mathrm{cut-off}}_{j} \wedge \qquad \dot{Q}^{\mathrm{set}}_{\mathrm{h},j} \ge \dot{Q}^{\mathrm{rated}}_{\mathrm{h},j} \\ 0 & \text{otherwise.} \end{cases} \tag{12}$$

The efficiency of the electric boiler η_{EB} is assumed to be constant, and operation is only limited by the rated power $\dot{Q}^{\mathrm{rated}}_{\mathrm{h,EB}}$, which serves as the design variable of the component. In contrast, a temperature-dependent efficiency - often referred to as the coefficient of performance (COP) - is used for the air-source heat pump. The COP is calculated using the inverse Carnot efficiency dependent on the ambient and supply cycle temperatures ($T_{\mathrm{amb}}, T_{\mathrm{supply}}$) and a performance factor ϵ_{HP}. In addition to the rated power, the cut-off temperature $T^{\mathrm{cut-off}}_{\mathrm{HP}}$ limits the heat pump's operation. The respective dispatch strategy determines the components' set-point power $\dot{Q}^{\mathrm{set}}_{\mathrm{h},j}$.

2.2.3 Energy storage: Both energy storage systems - battery and heat storage - are modeled according to the same modeling principle. This concept is explained below using the example of the battery storage. The following energy balance determines the SOE:

$$C^{\mathrm{rated}}_{\mathrm{B}} \cdot \frac{\mathrm{d}F_{\mathrm{B}}}{\mathrm{d}t} = \underbrace{-k^{\mathrm{sd}}_{\mathrm{B}} \cdot F_{\mathrm{B}} \cdot C^{\mathrm{rated}}_{\mathrm{B}}}_{\text{self-discharge losses}} + \underbrace{P_{\mathrm{B}} \cdot \begin{cases} \eta_{\mathrm{B}} & \text{if } P_{\mathrm{B}} \ge 0 \\ 1/\eta_{\mathrm{B}} & \text{if } P_{\mathrm{B}} < 0 \end{cases}}_{\text{charging/discharging}} \tag{13}$$

where F_{B} is the SOE, $k^{\mathrm{sd}}_{\mathrm{B}}$ is the self-discharge rate, and η_{B} is the respective charging and discharging efficiency. The self-discharge losses of the battery are determined via the constant self-discharge rate. For heat storage, on the other hand, the self-discharge losses are calculated using the temperature losses to the environment:

$$\dot{Q}_{\mathrm{h,loss}} = U_{\mathrm{loss,HS}} \cdot A_{\mathrm{HS}} \cdot (T_{\mathrm{HS}} - T_{\mathrm{amb}}) \,, \tag{14}$$

where U_{HS} is the heat loss coefficient, A_{HS} is the surface of the storage tank and T_{HS} is the uniform temperature in the storage tank. The rated energy capacity for the battery storage system $C^{\mathrm{rated}}_{\mathrm{B}}$ and the tank volume for the heat storage system V_{HS} are used as design variables. The thermal capacity of the heat storage $C^{\mathrm{rated}}_{\mathrm{HS}}$ can be determined directly via the tank volume, the water's specific heat capacity $c_{\mathrm{p,w}}$, and

 https://doi.org/10.52202/077185-0198

the water's density ρ_w. According to the operating limits for the SOE and the power, the battery power can be calculated as follows:

$$P_\mathrm{B} = \begin{cases} P_\mathrm{B}^\mathrm{max} & \text{if } 0 < F_\mathrm{B} < 1 \wedge \quad P_\mathrm{B}^\mathrm{set} > P_\mathrm{B}^\mathrm{max} \\ P_\mathrm{B}^\mathrm{set} & \text{if } 0 < F_\mathrm{B} < 1 \wedge -P_\mathrm{B}^\mathrm{max} \leq P_\mathrm{B}^\mathrm{set} \leq P_\mathrm{B}^\mathrm{max} \\ -P_\mathrm{B}^\mathrm{max} & \text{if } 0 < F_\mathrm{B} < 1 \wedge \quad P_\mathrm{B}^\mathrm{set} < -P_\mathrm{B}^\mathrm{max} \\ 0 & \text{otherwise.} \end{cases} \tag{15}$$

The power set-point $P_\mathrm{B}^\mathrm{set}$ is determined by the dispatch strategy, and the maximum power $P_\mathrm{B}^\mathrm{max}$ is calculated according to the technology-specific power factor Π_B.

Table 2: Technology-specific physical and operating parameters.

Battery	Heat pump	Electric boiler	Heat storage
$\eta_\mathrm{B} = 0.9487$	$\epsilon_\mathrm{HP} = 0.3$	$\eta_\mathrm{EB} = 1$	$\eta_\mathrm{HS} = 0.96$
$k_\mathrm{B}^\mathrm{sd} = 0.1\,\%/\mathrm{d}$	-	-	$U_\mathrm{loss,HS} = 0.354\,\mathrm{W/Km^2}$
$\Pi_\mathrm{B} = 1\,\mathrm{kW/kWh}$	$T_\mathrm{HP}^\mathrm{cutt-off} = 268.15\,\mathrm{K}$	-	$\Pi_\mathrm{B} = 1\,\mathrm{kW/kWh}$

2.3 Benchmark dispatch strategies

As shown in Figure 1, a dispatch strategy is used to determine the power set-point of the dispatchable components. Therefore, in the following section two rule-based dispatch strategies and an optimization problem to determine the optimal dispatch are presented.

2.3.1 Simple rule-based dispatch: A straightforward approach to dispatch flexible components is the use of priority order lists. Therefore, the electrical and heating components are categorized in separate priority order lists. Only the battery power set-point must be determined in the electrical supply system. For reasons of efficiency, the heat-supplying components are activated in the following sequence: 1. Heat pump, 2. electric boiler, and 3. heat storage:

$$P_\mathrm{B}^\mathrm{set} = -P_\mathrm{ED} + P_\mathrm{PV} - P_\mathrm{HP} - P_\mathrm{EB}, \tag{16}$$

$$\dot{Q}_\mathrm{h,HP}^\mathrm{set} = \dot{Q}_\mathrm{h,HD}, \tag{17}$$

$$\dot{Q}_\mathrm{h,EB}^\mathrm{set} = \dot{Q}_\mathrm{h,HD} - \dot{Q}_\mathrm{h,HP}, \tag{18}$$

$$\dot{Q}_\mathrm{h,HS}^\mathrm{set} = -\dot{Q}_\mathrm{h,HD} + \dot{Q}_\mathrm{h,HP} + \dot{Q}_\mathrm{h,EB}. \tag{19}$$

2.3.2 Advanced rule-based dispatch: The advanced rule-based dispatch strategy employs a state-machine framework to optimize the utilization of components, focusing on heat-driven components. The battery power set-point is calculated using the priority order list mentioned above (cf. eq. 16).

The strategy defines a state variable Z_j for each dispatchable component, determined by the temperature limits T_j^on and T_j^off. In state $Z_j = 0$, the component is turned off; in state $Z_j = 0.5$, the component is driven in part-load, and in state $Z_j = 1$, the component is driven in full load. The power set-point is then calculated as follows:

$$\dot{Q}_{\mathrm{h},j}^\mathrm{set} = \begin{cases} \dot{Q}_{\mathrm{h},j}^\mathrm{max} & \text{if } Z_j = 1 \\ \dot{Q}_{\mathrm{h},j}^\mathrm{max} \cdot \left(1 - 0.5 \cdot \frac{T_\mathrm{HS} - T_j^\mathrm{on}}{T_j^\mathrm{off} - T_j^\mathrm{on}}\right) & \text{if } Z_j = 0.5 \\ 0 & \text{if } Z_j = 0 \end{cases} \qquad \forall j \in \{\mathrm{HP, EB}\} \tag{20}$$

The power set-point of the heat storage is calculated according to eq. (17). Within this dispatch strategy, the temperature limits T_j^on and T_j^off are defined as additional optimization variables $\mathbf{x}_\mathrm{dispatch}$ and solved by the presented system optimization problem (cf. eq. 1).

https://doi.org/10.52202/077185-0198

2.3.3 Optimal dispatch: In addition to the use of rule-based dispatch strategies, the optimal power trajectory of the components can be determined directly via the optimal dispatch problem:

$$
\begin{aligned}
\underset{P_{\mathrm{B}},\dot{Q}_{\mathrm{h,HP}},\dot{Q}_{\mathrm{h,EB}},\dot{Q}_{\mathrm{h,HS}}}{\text{minimize}} \quad & J_{\mathrm{o}} && (21)\\
\text{subject to} \quad & 0 \leq F_{\mathrm{B}} \leq 1, && (22)\\
& T_{\mathrm{HS}}^{\min} \leq T_{\mathrm{HS}} \leq T_{\mathrm{HS}}^{\max}, && (23)\\
& P_{\mathrm{B}}^{\min} \leq P_{\mathrm{B}} \leq P_{\mathrm{B}}^{\max}, && (24)\\
& \dot{Q}_{\mathrm{h},j}^{\min} \leq \dot{Q}_{\mathrm{h},j} \leq \dot{Q}_{\mathrm{h},j}^{\max} \qquad \forall j \in \{\mathrm{HP,EB,HS}\}, && (25)\\
& 0 \leq \dot{Q}_{\mathrm{h,HP}} \cdot \left(T^{\mathrm{amb}} - T_{\mathrm{HP}}^{\mathrm{co}}\right), && (26)\\
& \text{eqs. (2) -(11)} \wedge \text{(13) - (14).}
\end{aligned}
$$

In this case, the power of the components is used directly as optimization variables. The operating limits of the individual components are not taken into account via the rule-based equations (cf. eqs. 12, 15) but are integrated directly as constraints (cf. eqs. 22 - 26). Equations (22) and (23) are used to limit the SOE of the storage units. Equations (24) and (25) are used to consider the power limits of the components, and eq. (26) considers the cut-off temperature of the air-source heat pump. In addition, as in the system design optimization above, the power balances, the cyclical SOE constraints, and the component models must also be considered.

In the other dispatch strategies, the dispatch variables are optimized directly in the system design optimization stage. Using the optimal dispatch approach, the system is optimized in two stages. The system design ($\mathbf{x}_{\mathrm{design}}$) and the initial values ($\mathbf{x}_{\mathrm{start}}$) are optimized on the first level using the heuristic algorithm presented in subsection 2.1. The optimal dispatch problem is solved in the underlying stage using the gradient-based *interior point optimization* (IPOPT) algorithm (Wächter and Biegler, 2006).

3 DISPATCH STRATEGY USING ARTIFICIAL NEURAL NETWORKS

This section introduces the dispatch using ANN. First, the operating method using ANN is explained. Then, the training method is presented.

3.1 Operating method

The ANN-based dispatch strategy comprises two control elements: The actual ANN and a clearing rule. The battery system and the heat pump are directly controlled by the set-point power determined by the ANN, denoted as $\mathbf{a}_{\mathrm{ANN}}$. A clearing rule-based set-point power, $\mathbf{a}_{\mathrm{CR}}$ is established for the electric boiler and the heat storage to ensure a reliable energy supply:

$$\dot{Q}_{\mathrm{h,HS}}^{\mathrm{set}} = -\dot{Q}_{\mathrm{h,HD}} + \dot{Q}_{\mathrm{h,HP}}, \tag{27}$$

$$\dot{Q}_{\mathrm{h,EB}}^{\mathrm{set}} = \dot{Q}_{\mathrm{h,HD}} - \dot{Q}_{\mathrm{h,HP}} - \dot{Q}_{\mathrm{h,HS}}. \tag{28}$$

This dual-component strategy facilitates efficient and reliable energy dispatch within the system.

3.2 Training method

The three-stage training framework for the neural networks is depicted in Figure 3. The optimal dispatch problem is initially solved to obtain the optimal trajectory of the actions $\mathbf{a}_{\mathrm{OD}}$ and corresponding observations $\mathbf{o}_{\mathrm{OD}}$. In the second step, the ANN is then trained to predict the optimal actions $\mathbf{a}_{\mathrm{OD}}$ based on the previously calculated observations $\mathbf{o}_{\mathrm{OD}}$. The deviation between the predicted action from the ANN $\mathbf{a}_{\mathrm{ANN}}$ and the optimal action serves as a training reward in this step:

$$r = \sum_{j \in \{\mathrm{HP,\,B}\}} \frac{\left|a_{\mathrm{OD},j} - a_{\mathrm{ANN},j}\right|}{a_j^{\max} - a_j^{\min}}. \tag{29}$$

https://doi.org/10.52202/077185-0198

This training step can be done quickly, but it does not evaluate the direct impact of the dispatch strategy on the energy system or the resulting costs. Therefore, it serves only as an initial solution $\mathbf{x}_{\text{ANN},0}$ for the third step. In this advanced stage, the ANN directly sets actions for dispatchable components in the energy system model and receives the corresponding observations by simulating the energy system model. Since system operation is simulated during training, the resulting annual operating cost can be used directly as a reward for the training algorithm. The heuristic algorithm *NeuroEvolution of Augmenting Topologies* is used as the training algorithm (McIntyre et al., 2023).

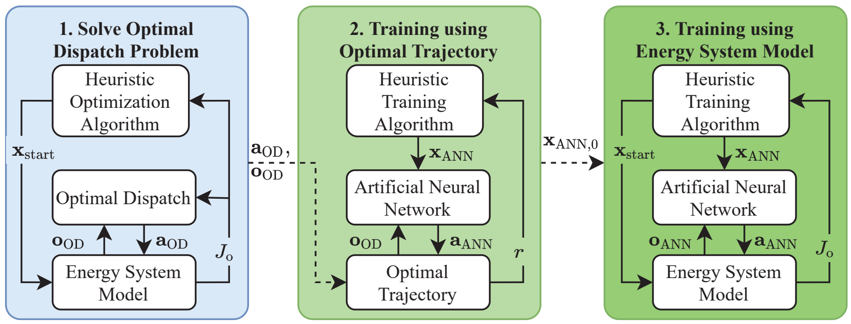

Figure 3: Schematic representation of the three-stage training framework for an ANN-based dispatch strategy. Step 1: Solve the optimal dispatch problem to calculate the optimal trajectory for action $\mathbf{a}_{\text{OD}}$ and observation $\mathbf{o}_{\text{OD}}$. Step 2: Train the ANN to predict the optimal action. Step 3: Train the ANN by simulating the observations and reward using the solution of step 2 as an initial solution $\mathbf{x}_{\text{ANN},0}$.

4 CASE STUDY

The following section presents the results of the case study. As depicted in Figure 4, the case study consist out of two parts. In the first part, subsection 4.1, the different dispatch strategies are compared using a fixed system design $\mathbf{x}_{\text{design},0}$. In the second part, subsection 4.2, the impact of the different dispatch strategies on the optimal system design is analyzed. Note that in the ANN-based approach, the optimization is performed iteratively - dispatch training with fixed design and design optimization with fixed ANN-based dispatch.

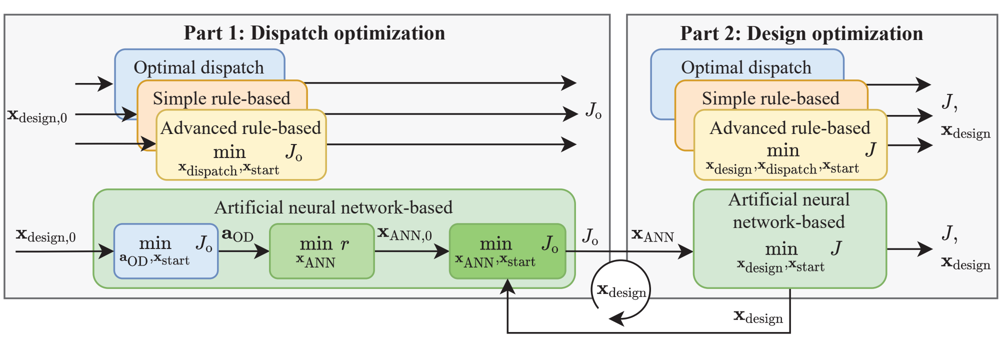

Figure 4: Graphical representation of the two-step analysis procedure: First, the comparison of different dispatch strategies using a fixed design $\mathbf{x}_{\text{design},0}$, and second, the comparison of the design optimization results using the different dispatch strategies.

https://doi.org/10.52202/077185-0198

4.1 Analysis Part 1: Dispatch optimization with fixed component design

For the first part of the analysis, the comparison of the dispatch strategies with predefined system design, only an overview is provided. Details of the analysis can be found in our ongoing research (Koenemann et al., 2024). Table 3 shows the predefined component design. In Figure 5, the resulting annual operating costs of the different dispatch strategies as a deviation from the annual operating costs using the optimal dispatch ($\Delta J_{\mathrm{o},i}$) are presented: On the left-hand side for the training data set and on the right-hand side for the test data set. The ANN-based dispatch strategy is significantly better than the two rule-based dispatch strategies for both data sets. The main reason for this is that more renewable energy is used for heat consumption via the heat pump with the help of the ANN-based dispatch strategy compared to the rule-based approaches. At the same time, the heat pump is also used more efficiently (higher ambient temperatures). However, it is essential to emphasize that the training time for learning the ANN-based dispatch strategy is significant, with around 9085 hours of computing time. Optimizing the advanced rule-based dispatch strategy requires only 28 hours of computing time. However, since the training can be parallelized on a high-performance cluster with approximately hundred cores in parallel, a total training of approx. 90.85 hours can be achieved. In addition, the training only needs to be carried out once. The network can then be evaluated instantly during operation.

Table 3: Predefined system design for part one of the case study.

Photovoltaic	Battery	Heat pump	Electric boiler	Heat storage
$P_{\mathrm{PV}}^{\mathrm{rated}}$	$C_{\mathrm{B}}^{\mathrm{rated}}$	$\dot{Q}_{\mathrm{h,HP}}^{\mathrm{rated}}$	$\dot{Q}_{\mathrm{h,EB}}^{\mathrm{rated}}$	V_{HS}
100 kW	30 kWh	40 kW	120 kW	11.51 m^3

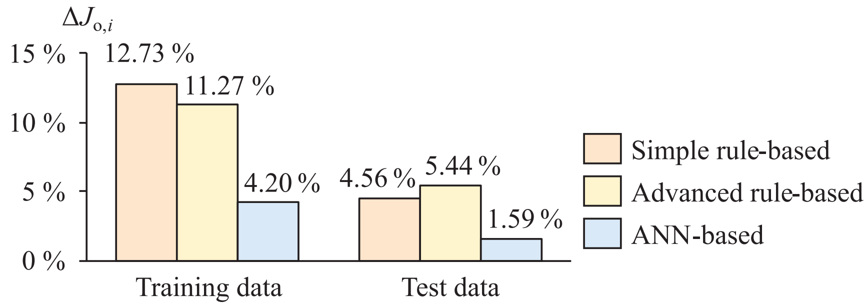

Figure 5: Comparison of the resulting annual operating costs as deviation from the optimal dispatch $\Delta J_{\mathrm{o},i}$ applying the different dispatch strategies on the training and test dataset.

4.2 Analysis Part 2: Design optimization

In the following section, the results of the system design optimization using the different dispatch strategies are presented. As shown in Figure 4, system optimization with the ANN-based dispatch strategy is carried out iteratively, i.e. training with fixed design and design optimization with fixed dispatch strategy are each carried out alternately in each case. The results of the individual steps can be seen on the left-hand side of Figure 6. The right-hand side shows the resulting system costs of the system optimization with the benchmark dispatch strategies. The lighter shade reflects the operating cost J_{o}, and the darker shade reflects the operating independent costs $J_{\mathrm{c,m}}$. The corresponding optimum component design applying the different dispatch strategies can be seen in Figure 7. Despite a comparatively poor initial design (about 15.87% worse than the optimal system cost with the simple rule-based design), the optimal ANN-based design outperforms the simple design by 9.19% and the advanced rule-based design by 5.80%. The main reasons for this are similar to those in the first part of the analysis. The ANN-based dispatch improves the utilization of the PV system by using the excess power with the heat pump and intermediate storage

https://doi.org/10.52202/077185-0198

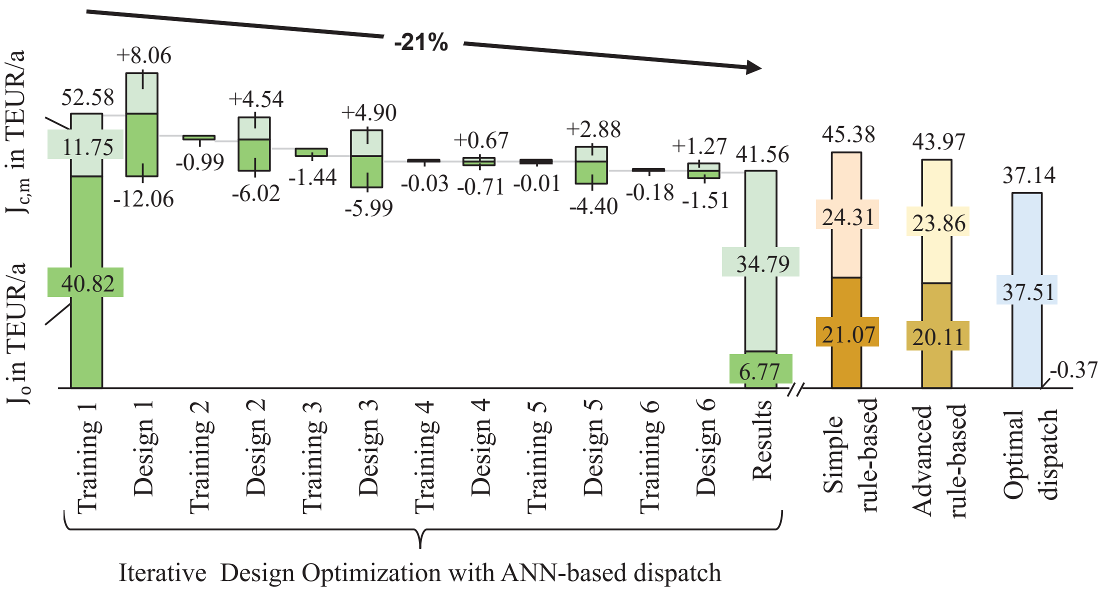

Figure 6: Resulting annual operating cost J_o and annual capital and maintenance cost $J_{c,m}$ of the system design optimization using the different dispatch strategies. On the left are the results of the iterative optimization of training with fixed design and design optimization with fixed ANN-based dispatch, on the right for the benchmark dispatch strategies.

in the heat storage to supply heat. This means that less expensive grid power is required, and the PV system is more economical and, therefore, sized more prominent. In order to make the best possible use of the temporary peaks of the PV system, the heat pump and the heat storage are also dimensioned larger than with the rule-based dispatch strategies. At the same time, installing an electric boiler is no longer required with the ANN-based dispatch. The design of the battery storage system is of a similar order of magnitude, as all dispatch strategies use the battery storage according to the same logic (temporary storage of the renewable surplus). With the ANN-based design and the optimal dispatch design, the rated capacity of the battery storage is slightly lower because, as already mentioned, the heat storage is also used to store the renewable surplus temporarily. The design with the optimal dispatch is similar to the ANN-based design, but the system costs are significantly lower. The optimal dispatch is calculated with the assumption of perfect forecasting. Therefore, the components can be operated even more efficiently. However, by assuming the perfect forecast, this solution cannot be implemented in real-time applications. Consequently, while this approach serves as a valuable benchmark, it should be appropriately oversized when installing the components in this manner.

5 CONCLUSION

In the present paper, a comparative analysis is performed to analyze the impact of dispatch strategy on the system operation and design optimization of DES. An ANN-based dispatch strategy trained with a three-stage training process is compared with two rule-based dispatch strategies and the optimal dispatch, on the one hand, using an already predefined system, and, on the other hand, directly when applied in system design optimization.

The comparison of dispatch strategies with a fixed design shows that the ANN-based dispatch strategy performs significantly better than the rule-based approaches (6.78% and 3.79%) and only slightly worse than the optimal dispatch (4.20 %). In addition, the learned dispatch strategy outperforms the rule-based dispatch strategies by applying an independent test data set.

https://doi.org/10.52202/077185-0198

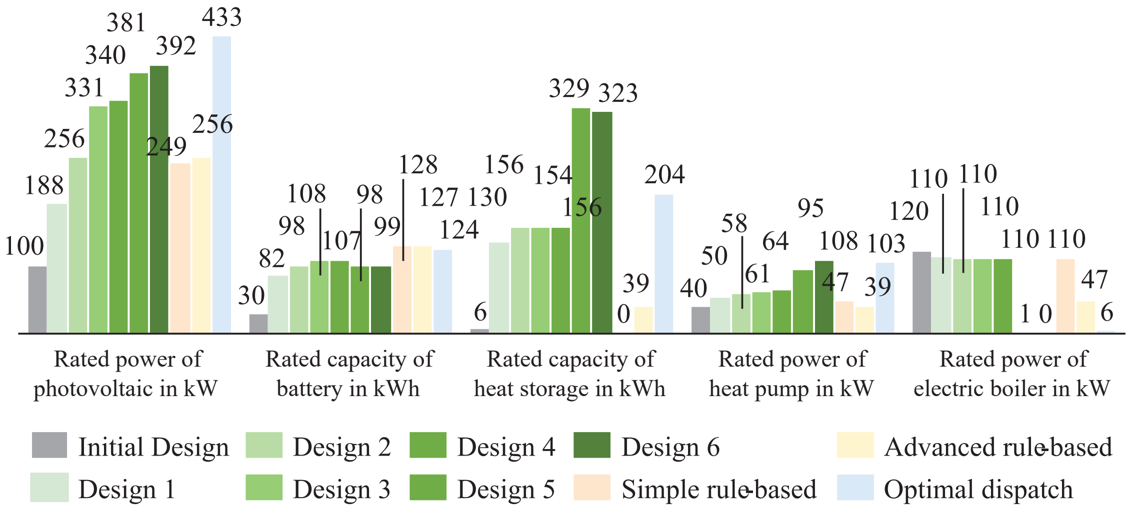

Figure 7: Resulting optimal design of the optimization using the different dispatch strategies.

The results are similar for system design optimization. Although the ANN-based design is carried out iteratively (training with fixed design and design optimization with fixed dispatch), the ANN-based design outperforms the simple design by 9.19% and the advanced rule-based design by 5.80%. Since a perfect forecast is assumed for optimal dispatch, this operation results in the lowest costs (10.63% better than the ANN-based). However, this solution should only be considered a benchmark since this dispatch cannot be applied in real-world systems.

The analysis also showed that not only does the optimal system cost depend on the dispatch strategy, but the optimal design of each component also varies depending on the dispatch strategy applied. For example, the ANN-based dispatch strategy utilizes the PV system via the heat pump and heat storage more economically than the rule-based strategies. For this reason, these three components are designed to be larger than in the rule-based dispatch design. On the other hand, in contrast to the rule-based design, the inefficient electric boiler is not required in the ANN-based design. The optimal dispatch design is similar to the ANN-based design.

The study is limited by its reliance on a simplified model for comparison, which may not capture the complex realities of DES. Future research should include evaluations against alternative dispatch methods (e.g., MPC), developing more sophisticated models, and validating real-world data to improve the robustness and applicability of ANN-based dispatch strategies. Furthermore, only iterative design optimization is considered in this study. In the future, it would be interesting to see whether even better results can be obtained by coupling design and scheduling optimization with ANN.

NOMENCLATURE

ANN Artificial Neural Networks
B Li-ion Battery storage
DES Decentralized Energy System
EB Electric Boiler
ED Electrical Demand
EG Electrical Grid
HP Heat Pump
HS Heat Storage
HD Heat Demand
PV Photovoltaic system
SOE State of Energy
TAC Total Annual Cost *J*

https://doi.org/10.52202/077185-0198

REFERENCES

Biscani, F. and D. Izzo (2010). “A Parallel Global Multiobjective Framework for Optimization: Pagmo”. In: *JOSS* 5.53, p. 2338.

Bundesverband der Energie- und Wasserwirtschaft (July 2023). *BDEW-Strompreisanalyse Juli 2023: Haushalte Und Industrie*.

Cybenko, G. (Dec. 1989). “Approximation by Superpositions of a Sigmoidal Function”. In: *Math. Control Signal Systems* 2.4, pp. 303–314. (Visited on 03/06/2024).

Domínguez-Barbero, D. et al. (June 2020). “Optimising a Microgrid System by Deep Reinforcement Learning Techniques”. In: *Energies* 13.11, p. 2830. (Visited on 02/22/2023).

Federal Government Germany (2016). *Gesetz Zur Einführung von Ausschreibungen Für Strom Aus Erneuerbaren Energien Und Zu Weiteren Änderungen Des Rechts Der Erneuerbaren Energien*. (Visited on 10/12/2023).

Geyer, P. and S. Singaravel (Oct. 2018). “Component-Based Machine Learning for Performance Prediction in Building Design”. In: *Applied Energy* 228, pp. 1439–1453. (Visited on 06/13/2023).

Jin, R. et al. (Dec. 2022). “Deep Reinforcement Learning-Based Strategy for Charging Station Participating in Demand Response”. In: *Applied Energy* 328, p. 120140. (Visited on 07/13/2023).

Koenemann, L. et al. (2024). “Dispatch of Decentralized Energy Systems Using Artificial Neural Networks: A Comparative Analysis with Emphasis on Training Methods”.

Kost, C. (June 2021). *Studie: Stromgestehungskoten Erneuerbarer Energien*. Tech. rep. Frauenhofer ISE.

Kotzur, L. et al. (2018). “Impact of Different Time Series Aggregation Methods on Optimal Energy System Design”. In: *Renewable Energy* 117, pp. 474–487.

McIntyre, A. et al. (2023). *Neat-Python*.

McKenna, E. and M. Thomson (Mar. 2016). “High-Resolution Stochastic Integrated Thermal–Electrical Domestic Demand Model”. In: *Applied Energy* 165, pp. 445–461. (Visited on 02/21/2023).

Ministerium für Umwelt, Klima und Energiewirtschaft Baden-Württemberg (2023). *Technikkatalog Zur Kommunalen Wärmeplanung*. (Visited on 05/03/2023).

Murray, P., K. Orehounig, and J. Carmeliet (Feb. 2019). “Optimal Design of Multi-Energy Systems at Different Degrees of Decentralization”. In: *Energy Procedia* 158, pp. 4204–4209. (Visited on 02/21/2024).

Open Source Modelica Consortium (2022). *OpenModelica Homepage*. https://www.openmodelica.org/.

Perera, A. et al. (June 2019). “Machine Learning Methods to Assist Energy System Optimization”. In: *Applied Energy* 243, pp. 191–205. (Visited on 04/28/2023).

– (Mar. 2020). “Introducing Reinforcement Learning to the Energy System Design Process”. In: *Applied Energy* 262, p. 114580. (Visited on 02/23/2023).

Pfenninger, S. and I. Staffell (2016). “Long-Term Patterns of European PV Output Using 30 Years of Validated Hourly Reanalysis and Satellite Data”. In: *Energy* 114, pp. 1251–1265.

Qiu, Y. et al. (July 2023). “Local Integrated Energy System Operational Optimization Considering Multi-type Uncertainties: A Reinforcement Learning Approach Based on Improved TD3 Algorithm”. In: *IET Renewable Power Gen* 17.9, pp. 2236–2256. (Visited on 07/13/2023).

Rahman Fahim, S. et al. (July 2020). “Microgrid Fault Detection and Classification: Machine Learning Based Approach, Comparison, and Reviews”. In: *Energies* 13.13, p. 3460. (Visited on 02/22/2023).

Reynolds, J. et al. (Feb. 2019). “Operational Supply and Demand Optimisation of a Multi-Vector District Energy System Using Artificial Neural Networks and a Genetic Algorithm”. In: *Applied Energy* 235, pp. 699–713. (Visited on 02/22/2023).

Schmeling, L. et al. (Nov. 2022). “A Generalised Optimal Design Methodology for Distributed Energy Systems”. In: *Renewable Energy* 200, pp. 1223–1239. (Visited on 05/04/2023).

Stadler, P., A. Ashouri, and F. Maréchal (May 2016). “Model-Based Optimization of Distributed and Renewable Energy Systems in Buildings”. In: *Energy and Buildings* 120, pp. 103–113. (Visited on 02/24/2023).

Urbanucci, L. and D. Testi (2018). “Optimal Integrated Sizing and Operation of a CHP System with Monte Carlo Risk Analysis for Long-Term Uncertainty in Energy Demands”. In: *Energy Conversion and Management* 157, pp. 307–316.

Wächter, A. and L. T. Biegler (2006). “On the Implementation of an Interior-Point Filter Line-Search Algorithm for Large-Scale Nonlinear Programming”. In: *Math. Program.* 106.1, pp. 25–57.

Wang, Z. and T. Hong (July 2020). “Reinforcement Learning for Building Controls: The Opportunities and Challenges”. In: *Applied Energy* 269, p. 115036. (Visited on 05/04/2023).

Wilke, C. (2020). *Optimale Dimensionierung von Dezentralen, Regenerativen Energieversorgungssystemen in Quartieren*. Tech. rep. Hannover : Institutionelles Repositorium der Leibniz Universität Hannover.

https://doi.org/10.52202/077185-0198